

Article

Adaptive Event-Triggered Control Strategy for Ensuring Predefined Three-Dimensional Tracking Performance of Uncertain Nonlinear Underactuated Underwater Vehicles

Jin Hoe Kim and Sung Jin Yoo *

School of Electrical and Electronics Engineering, Chung-Ang University, 84 Heukseok-Ro, Dongjak-Gu, Seoul 06974, Korea; qhqo503@cau.ac.kr

* Correspondence: sjyoo@cau.ac.kr

Abstract: This paper presents an adaptive event-triggered control strategy for guaranteeing predefined tracking performance of uncertain nonlinear underactuated underwater vehicles (UUVs) in the three-dimensional space. Compared with the related results in the literature, the main contribution of this paper is to develop a nonlinear error transformation approach for ensuring predefined three-dimensional tracking performance under the underactuated property of 6-DOF UUVs and limited network resources. A nonlinear tracking error function is designed using a linear velocity rotation matrix and a time-varying performance function. An adaptive event-triggered control scheme using the nonlinear tracking error function and neural networks is constructed to ensure the practical stability of the closed-loop system with predefined three-dimensional tracking performance. In the proposed control scheme, auxiliary stabilizing signals are designed to resolve the underactuated problem of UUVs. Simulation results are presented to illustrate the effectiveness of the theoretical methodology.

Keywords: nonlinear error transformation; event-triggered tracking; predefined three-dimensional tracking performance; neural networks; underactuated underwater vehicles (UUVs)



Citation: Kim, J.H.; Yoo, S.J. Adaptive Event-Triggered Control Strategy for Ensuring Predefined Three-Dimensional Tracking Performance of Uncertain Nonlinear Underactuated Underwater Vehicles. *Mathematics* **2021**, *9*, 137. <https://doi.org/10.3390/math9020137>

Received: 21 December 2020

Accepted: 7 January 2021

Published: 10 January 2021

Publisher's Note: MDPI stays neutral with regard to jurisdictional claims in published maps and institutional affiliations.



Copyright: © 2021 by the authors. Licensee MDPI, Basel, Switzerland. This article is an open access article distributed under the terms and conditions of the Creative Commons Attribution (CC BY) license (<https://creativecommons.org/licenses/by/4.0/>).

1. Introduction

Control of nonlinear underwater vehicles is attracting much research attention recently, due to its practical application in submarine survey, exploration, oceanographic mapping, and region search for deep-sea wrecks [1–6]. The initial studies have focused on the planar or depth control design of underwater vehicles in the two-dimensional space [7–11]. However, these studies in the two-dimensional space provide limited solutions to various tracking problems in the practical three-dimensional underwater environment. For more practical application, three-dimensional control approaches have been studied for nonlinear underwater vehicles described by 5-degrees-of-freedom (5-DOF) or 6-DOF kinematics and dynamics. In [12], a path following controller was designed for 5-DOF underwater vehicles with ocean current disturbances. A ocean current observer to detect an external current was designed for trajectory tracking of 5-DOF underactuated underwater vehicles (UUVs) [13]. In [14,15], fuzzy-based or neural-network control techniques were developed for uncertain 5-DOF UUVs with external disturbances. To deal with uncertain 6-DOF models with the roll motion, three-dimensional trajectory tracking control designs were developed using several control techniques such as backstepping control [16,17] and sliding mode control [18]. However, in the aforementioned results, the transient and steady-state performance metrics of tracking errors cannot be designed a priori. To preselect the tracking performance metrics of underwater vehicles, the prescribed performance design technique [19] has been combined with the control methodologies of underwater vehicles [20–23]. In [21], a region tracking controller with predefined transient performance was designed for fully actuated underwater vehicles in presence of an ocean current and a thruster fault. Neural-network-based prescribed performance control designs were investigated for uncertain

5-DOF UUVs [22] and 6-DOF fully actuated underwater vehicles [20]. In [23], a prescribed performance control design was developed for 6-DOF UUVs. Despite these efforts, the controllers designed in [20–23] should be continuously updated and thus cannot be used in the network-based control environment with limited communication bandwidth. Since underwater acoustic communication has limited bandwidth, low propagation speed, and high energy consumption, the data transmission for the network-based control should be kept to a minimum amount [24]. Thus, it is significant to investigate an event-triggered control design issue for ensuring predefined three-dimensional tracking performance under the underactuated property of 6-DOF UUVs and limited network resources.

Event-triggered control strategies have been proposed to address control problems of linear and nonlinear systems under capacity-limited networks [25–28]. In the event-triggered control, the signal transmission burden can be reduced in the communication network because control inputs are executed only when certain triggering conditions are satisfied. Owing to this advantage, adaptive event-triggered control approaches have been actively developed for uncertain nonlinear systems [29–32]. However, the event-triggered control of underwater vehicles was only studied to design a depth controller in the two-dimensional space [33]. To the best of our knowledge, no studies have been reported thus far on the event-triggered control problem for ensuring predefined three-dimensional tracking performance of uncertain 6-DOF UUVs.

On the basis of the above discussion, the purpose of this paper is to present an adaptive event-triggered control strategy with predefined three-dimensional tracking performance for uncertain nonlinear 6-DOF UUVs. It is assumed that all nonlinearities in the dynamics of the UUV are unknown. Compared with the related results [20–23,33] in the literature, the main contribution of this study is to develop an error-transformation-based adaptive event-triggered tracking law for achieving predefined three-dimensional tracking performance while overcoming the underactuated problem of the nonlinear 6-DOF dynamics. To this end, a nonlinearly transformed tracking error function using a linear velocity rotation matrix and a time-varying performance function is presented. A neural-network-based adaptive event-triggered control scheme is recursively designed to ensure predefined three-dimensional tracking performance of the uncertain UUV where neural networks are employed to approximate unknown nonlinearities. In the proposed control scheme, auxiliary stabilizing signals using neural networks are derived to deal with the underactuated control design problem. We rigorously prove that the resulting event-triggered tracker ensures the practical stability of the closed-loop system and the exclusion of Zeno behavior.

The rest of this paper is outlined as follows. In Section 2, we introduce the 6-DOF kinematics and dynamics of uncertain nonlinear UUVs and formulate the predefined three-dimensional tracking performance control problem. A neural-network-based adaptive event-triggered tracker is constructed using the nonlinearly transformed tracking error function and the auxiliary stabilizing signals, and the closed-loop stability is analyzed in Section 3. Simulation studies are given in Section 4. Finally, we conclude in Section 5.

2. Problem Formulation

The kinematics for the position and attitude of an UUV can be described by

$$\begin{aligned}\dot{\eta} &= R_1(\zeta)v \\ \dot{\zeta} &= R_2(\zeta)\omega\end{aligned}\quad (1)$$

where $\eta = [x, y, z]^T$; x , y , and z are the positions of the center of gravity in an inertial coordinate frame, $\zeta = [\phi, \theta, \psi]^T$; ϕ , θ , and ψ denote roll, pitch, and yaw angles, respectively, $v = [u, v, w]^T$; u , v , and w are surge, sway, and heave velocities, respectively, and $\omega = [p, q, r]^T$; p , q , and r denote the roll, pitch, and yaw angular velocities in the body-fixed

frame, respectively. Here, the linear velocity rotation matrix $R_1(\zeta)$ and the angular velocity transformation matrix $R_2(\zeta)$ are given by

$$R_1(\zeta) = \begin{bmatrix} c_\theta c_\psi & s_\theta c_\psi s_\phi - s_\psi c_\phi & s_\theta c_\psi c_\phi + s_\psi s_\phi \\ c_\theta s_\psi & s_\theta s_\psi s_\phi + c_\psi c_\phi & s_\theta s_\psi c_\phi - c_\psi s_\phi \\ -s_\theta & c_\theta s_\phi & c_\theta c_\phi \end{bmatrix}$$

$$R_2(\zeta) = \begin{bmatrix} 1 & t_\theta s_\phi & t_\theta c_\phi \\ 0 & c_\phi & -s_\phi \\ 0 & s_\phi/c_\theta & c_\phi/c_\theta \end{bmatrix}$$

with $s(\cdot) = \sin(\cdot)$, $c(\cdot) = \cos(\cdot)$, and $t(\cdot) = \tan(\cdot)$. The structure of the neutrally buoyant UUV concerned in this paper is depicted in Figure 1.

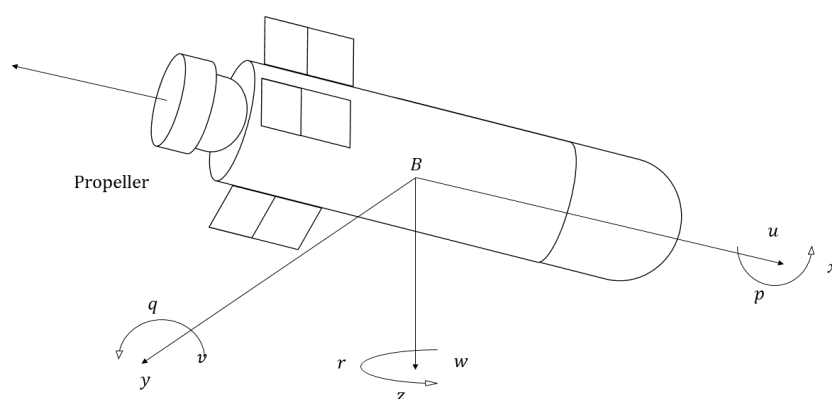


Figure 1. The structure of the UUV.

The dynamics of the UUV is given by

$$M \begin{bmatrix} \dot{v} \\ \dot{\omega} \end{bmatrix} = C(v, \omega) + G(\zeta) + \tau \tag{2}$$

where $M = M_1 + M_2$; $M_1 \in \mathbb{R}^{6 \times 6}$ and $M_2 \in \mathbb{R}^{6 \times 6}$ are the matrix of the rigid-body mass and the added mass, respectively, $C(v, \omega) \in \mathbb{R}^6$ is a vector derived by the Coriolis and damping matrices, $G(\zeta) \in \mathbb{R}^6$ is a vector induced from the gravitation and the buoyancy of the UUV, and $\tau = [\tau_X, \tau_Y, \tau_Z, \tau_K, \tau_M, \tau_N]$ is a vector denoting the control forces and moments. In this paper, the torpedo-shaped UUV model is considered to deal with the tracking problem. The torpedo-shaped UUV cannot move directly to the y - or z -direction in the body reference frame and the roll movement is undesirable in the practical UUV [34]. Thus, the underactuated torque vector $\tau = [\tau_X, 0, 0, 0, \tau_M, \tau_N]$ is considered in this paper. The detailed definitions of M , C , and G are presented in Appendix A. For more details for the model of UUVs, see [35,36].

Assumption 1. The nonlinear function vectors $C(v, \omega)$ and $G(\zeta)$ are unknown for the control design.

Assumption 2. The desired three-dimensional trajectory $\eta_d \in \mathbb{R}^3$ and its derivatives $\dot{\eta}_d \in \mathbb{R}^3$ and $\ddot{\eta}_d \in \mathbb{R}^3$ are bounded.

Problem 1. Our problem is to design an adaptive event-triggered control law τ for ensuring predefined three-dimensional tracking performance of the uncertain UUV described by (1) and (2) so that the position trajectory η of the UUV follows the desired trajectory η_d in the three-dimensional space.

3. Adaptive Event-Triggered Control with Predefined Three-Dimensional Tracking Performance

In this section, an adaptive event-triggered control methodology using an error transformation function and stabilizing auxiliary signals is established to ensure predefined three-dimensional tracking performance of the UUV. The dynamic surface design procedure using the predefined performance concept is derived step by step.

Step 1: Let us consider the kinematics (1) and define the position errors $s = [s_1, s_2, s_3]^T = \eta - \eta_d$. Then, to ensure predefined three-dimensional tracking performance under the underactuated property, we define the nonlinearly transformed error surface $\Gamma_1 = [\Gamma_{1,1}, \Gamma_{1,2}, \Gamma_{1,3}]^T$ as

$$\Gamma_1 = R_1^{-1}(\zeta)\Phi - \rho \tag{3}$$

where $\Phi = [\Phi_1, \Phi_2, \Phi_3]^T$, and $\rho = [\varrho, 0, 0]^T$ denotes the radius of error surface with the design constant ϱ . Here, the design constant ϱ is selected relatively small compared to the length of the UUV, and $\Phi_i, i = 1, 2, 3$, is defined as

$$\Phi_i\left(\frac{s_i}{\mu_i}\right) = \ln\left(\frac{\delta_{1,i}\delta_{2,i} + \delta_{2,i}(s_i/\mu_i)}{\delta_{1,i}\delta_{2,i} - \delta_{1,i}(s_i/\mu_i)}\right) \tag{4}$$

where $0 < \delta_{1,i} \leq 1$ and $0 < \delta_{2,i} \leq 1$ are design constants, and $\mu_i(t) = (\mu_{i,0} - \mu_{i,\infty})e^{-g_i t} + \mu_{i,\infty}$ is the performance function with design parameters $g_i > 0, \mu_{i,0} > 0$, and $\mu_{i,\infty} > 0$ satisfying $\mu_{i,0} > \mu_{i,\infty}$ and $-\delta_{1,i}\mu_i(0) < s_i(0) < \delta_{2,i}\mu_i(0)$.

Lemma 1. *If $\Gamma_{1,i} \in \mathcal{L}_\infty, -\delta_{1,i}\mu_i(t) < s_i(t) < \delta_{2,i}\mu_i(t)$ is ensured for all $t \geq 0$ where $i = 1, 2, 3$.*

Proof. Let us define $\Theta = R_1(\zeta)(\Gamma_1 + \rho)$ where $\Theta = [\Theta_1, \Theta_2, \Theta_3]^T$. From the definition of $R_1(\zeta)$, there exists a constant \bar{R}_1 such that $\|R_1(\zeta)\| \leq \bar{R}_1$. Then, from $\Gamma_{1,i} \in \mathcal{L}_\infty, \Theta_i$ are bounded where $i = 1, 2, 3$. Thus, there exist constants $\underline{\Theta}_i$ and $\bar{\Theta}_i$ such that $\underline{\Theta}_i < \Theta_i(t) < \bar{\Theta}_i, \forall t \geq 0$. Using the bijective property $\Phi_i : (-\delta_{1,i}, \delta_{2,i}) \mapsto (-\infty, \infty)$ [37], it holds that $\Phi_i^{-1}(\underline{\Theta}_i) < s_i/\mu_i < \Phi_i^{-1}(\bar{\Theta}_i)$. Owing to $-\delta_{1,i} < \Phi_i^{-1} < \delta_{2,i}$, we have $-\delta_{1,i}\mu_i(t) < s_i(t) < \delta_{2,i}\mu_i(t)$ for all $t \geq 0$. \square

Remark 1. *In (3), $R_1^{-1}(\zeta)$ and ρ are combined with the nonlinear error function vector Φ in order to design the underactuated control scheme with the predefined three-dimensional tracking performance. From Lemma 1, the boundedness of the error surface vector leads to the satisfaction of the inequality $-\delta_{1,i}\mu_i(t) < s_i(t) < \delta_{2,i}\mu_i(t)$ for all $t \geq 0$ where $i = 1, 2, 3$. That is, the bounds of the transient and steady-state performance of the position errors $s_i(t)$ can be predefined by selecting the design parameters $\delta_{1,i}, \delta_{2,i}$, and functions $\mu_i(t)$. Thus, the predefined three-dimensional tracking performance is ensured provided that $\Gamma_{1,i} \in \mathcal{L}_\infty$. Accordingly, the primary focus of this study is to design an adaptive event-triggered control scheme for ensuring the boundedness of $\Gamma_{1,i}$.*

The time derivative of Γ is represented by

$$\begin{aligned} \dot{\Gamma}_1 &= \dot{R}_1^{-1}(\zeta)\Phi + R_1^{-1}(\zeta)\dot{\Phi} \\ &= -K(\Gamma_1 + \rho) + R_1^{-1}A(\dot{\eta} - \dot{\eta}_d - \dot{\mu}\mu^{-1}s_1) \end{aligned} \tag{5}$$

where $K = -\dot{R}_1^{-1}R_1, A = \text{diag}[A_1, A_2, A_3]$ with $A_i = (1/(s_i + \delta_{1,i}\mu_i)) - (1/(s_i - \delta_{2,i}\mu_i)), i = 1, 2, 3$, and $\mu = \text{diag}[\mu_1, \mu_2, \mu_3]$. Here, $\text{diag}[\cdot]$ is the diagonal matrix.

Then, we have

$$K = -\dot{R}_1^{-1}R_1 = \begin{bmatrix} 0 & -r & q \\ r & 0 & -p \\ -q & p & 0 \end{bmatrix}. \tag{6}$$

Using (6), we obtain that

$$\begin{aligned} \dot{\Gamma}_1 &= -K\Gamma_1 - K\rho + R_1^{-1}AR_1v - R_1^{-1}A(\dot{\eta}_d + \dot{\mu}\mu^{-1}s_1) \\ &= -K\Gamma_1 - \begin{bmatrix} 0 & -r & q \\ r & 0 & -p \\ -q & p & 0 \end{bmatrix} \begin{bmatrix} \varrho \\ 0 \\ 0 \end{bmatrix} + H \begin{bmatrix} u \\ v \\ w \end{bmatrix} - R_1^{-1}A(\dot{\eta}_d + \dot{\mu}\mu^{-1}s_1) \\ &= -K\Gamma_1 + N \begin{bmatrix} u \\ q \\ r \end{bmatrix} + H \begin{bmatrix} 0 \\ v \\ w \end{bmatrix} - R_1^{-1}A(\dot{\eta}_d + \dot{\mu}\mu^{-1}s_1) \end{aligned} \tag{7}$$

where $H = R_1^{-1}AR_1$ and

$$N = \begin{bmatrix} H_{1,1} & 0 & 0 \\ H_{2,1} & 0 & -\varrho \\ H_{3,1} & \varrho & 0 \end{bmatrix}.$$

Here, $H_{m,n}$ means the (m, n) element of the matrix H .

Using the dynamic surface design concept [38], we define the error surface vector $e = [e_u, e_q, e_r]^T$ with $e_u = u - \bar{\alpha}_u$, $e_q = q - \bar{\alpha}_q$, and $e_r = r - \bar{\alpha}_r$, and the boundary layer error vector $c = [c_1, c_2, c_3] = \bar{\alpha} - \alpha$ where $\alpha = [\alpha_u, \alpha_q, \alpha_r]^T$ is the virtual control vector and $\bar{\alpha} = [\bar{\alpha}_u, \bar{\alpha}_q, \bar{\alpha}_r]^T$ is the filtered signal vector of virtual control laws α_u , α_q , and α_r that is obtained by the first-order low-pass filter

$$\zeta \dot{\bar{\alpha}} + \bar{\alpha} = \alpha, \quad \bar{\alpha}(0) = \alpha(0) \tag{8}$$

where $\zeta > 0$ is the small constant.

Using the error surface vector e and the boundary layer error c , (7) becomes

$$\dot{\Gamma}_1 = -K\Gamma_1 + N(e + \alpha + c) + H \begin{bmatrix} 0 \\ v \\ w \end{bmatrix} - R_1^{-1}A(\dot{\eta}_d + \dot{\mu}\mu^{-1}s_1). \tag{9}$$

The virtual control vector $\alpha = [\alpha_u, \alpha_q, \alpha_r]^T$ is presented as

$$\alpha = N^{-1} \left(-\gamma_1\Gamma_1 - H \begin{bmatrix} 0 \\ v \\ w \end{bmatrix} + R_1^{-1}A(\dot{\eta}_d + \dot{\mu}\mu^{-1}s_1) \right) \tag{10}$$

where $\gamma_1 = \text{diag}[\gamma_{1,1} \ \gamma_{1,2} \ \gamma_{1,3}]$; $\gamma_{1,i}$, $i = 1, \dots, 3$, are positive constants.

Substituting (10) to (9) gives

$$\dot{\Gamma}_1 = -K\Gamma_1 - \gamma_1\Gamma_1 + N(e + c). \tag{11}$$

We choose a Lyapunov function $V_1 = \Gamma_1^T\Gamma_1/2$. Then, the time derivative of V_1 is represented by

$$\dot{V}_1 = -\Gamma_1^T\gamma_1\Gamma_1 + \Gamma_1^TN(e + c). \tag{12}$$

where $\Gamma_1^TK\Gamma_1 = 0$ due to the skew symmetric matrix K .

Step 2: To design the underactuated torque vector $\tau = [\tau_X, 0, 0, 0, \tau_M, \tau_N]$, we define the error surface vector $\Gamma_2 = [\Gamma_{2,1}, \dots, \Gamma_{2,6}]^T = \omega - \chi$ where $\omega = [v^T, \omega^T]^T$ and $\chi = [\bar{\alpha}_u, \beta_1, \beta_2, \beta_3, \bar{\alpha}_q, \bar{\alpha}_r]^T$. Here, β_1 , β_2 , and β_3 in χ are the auxiliary stabilizing signals to be designed later.

Using (2), the time derivative of Γ_2 is obtained as

$$\dot{\Gamma}_2 = M^{-1}(F(\omega, \zeta) + \tau) - \dot{\chi} \tag{13}$$

where $F(\omega, \zeta) = C(\omega) + G(\zeta)$.

For the online approximation of unknown nonlinear function vector $F(\omega, \zeta)$, radial basis function neural networks [39] are employed. Then, F can be approximated over the compact set Y as follows

$$F(\bar{x}) = W^*{}^\top \Omega(\bar{x}) + \varepsilon \tag{14}$$

where $\bar{x} = [\omega^\top, \zeta^\top]^\top \in Y \subset \mathbb{R}^6$ denotes the input vector of radial basis function neural networks, the optimal weighting matrix W^* is defined as $W^* = \text{diag}[W_1^*, \dots, W_6^*]$ satisfying $\|W^*\|_F \leq \bar{W}$ with an unknown constant $\bar{W} > 0$, $W_f^* = [W_{f,1}^*, \dots, W_{f,n}^*]^\top$ with $f = 1, \dots, 6$, $\|\cdot\|_F$ is the Frobenius norm, Ω denotes the Gaussian function vector $\Omega = [\Omega_1^\top, \dots, \Omega_6^\top]^\top$; $\Omega_f = [\Omega_{f,1}, \dots, \Omega_{f,n}]^\top$ with $f = 1, \dots, 6$, and $\varepsilon \in \mathbb{R}^6$ is a reconstruction error vector such as $\|\varepsilon\| \leq \bar{\varepsilon}$ with an unknown constant $\bar{\varepsilon} > 0$.

An adaptive event-triggered tracking law is presented as

$$\tau(t) = \check{\tau}(t_j), \quad \forall t \in [t_j, t_{j+1}) \tag{15}$$

$$t_{j+1} = \inf\{t > t_j \mid \|S_\tau(t)\| \geq \kappa_1 \|e(t)\| + \kappa_2\} \tag{16}$$

where t_j denotes the update time of the control torque τ with $j \in \mathbb{Z}^+$, $S_\tau(t) = \check{\tau}(t) - \tau(t)$, and $\kappa_1 > 0$ and $\kappa_2 > 0$ are design constants. When the event-triggering condition (16) is satisfied, the tracking law τ is updated at t_{j+1} and is set to $\check{\tau} = [\check{\tau}_1, 0, 0, 0, \check{\tau}_5, \check{\tau}_6]^\top$ given by

$$\begin{bmatrix} \check{\tau}_1 \\ \check{\tau}_5 \\ \check{\tau}_6 \end{bmatrix} = -\bar{\gamma}_{2,1}e + \begin{bmatrix} B_1 \\ B_5 \\ B_6 \end{bmatrix} - \begin{bmatrix} \hat{W}_1^\top \Omega_1 \\ \hat{W}_5^\top \Omega_5 \\ \hat{W}_6^\top \Omega_6 \end{bmatrix} - (\hat{\varepsilon} + \kappa_2) \tanh\left(\frac{e}{\vartheta}\right) - \kappa_1 e - N^\top \Gamma_1 \tag{17}$$

where $\bar{\gamma}_{2,1} = \text{diag}[\gamma_{2,1}, \gamma_{2,5}, \gamma_{2,6}]$; $\gamma_{2,1}$, $\gamma_{2,5}$, and $\gamma_{2,6}$ denote positive design parameters, \hat{W}_1 , \hat{W}_5 , and \hat{W}_6 are estimates of W_1^* , W_5^* , and W_6^* , respectively, $\tanh(e/\vartheta) = [\tanh(\Gamma_{2,1}/\vartheta), \tanh(\Gamma_{2,5}/\vartheta), \tanh(\Gamma_{2,6}/\vartheta)]^\top$ with a constant $\vartheta > 0$, and $\hat{\varepsilon}$ denotes an estimate of $\bar{\varepsilon}$. Here, B_1 , B_5 , B_6 are elements of the vector $B = [B_1, \dots, B_6]^\top = M\chi$ with $\chi = [(\alpha_u - \bar{\alpha}_u)/\zeta, \dot{\beta}_1, \dot{\beta}_2, \dot{\beta}_3, (\alpha_q - \bar{\alpha}_q)/\zeta, (\alpha_r - \bar{\alpha}_r)/\zeta]^\top$. The dynamics of the auxiliary stabilizing signals β_1 , β_2 , and β_3 are designed as

$$\begin{bmatrix} \dot{\beta}_1 \\ \dot{\beta}_2 \\ \dot{\beta}_3 \end{bmatrix} = \bar{M}_2^{-1} \left(\bar{\gamma}_{2,2} \begin{bmatrix} \Gamma_{2,2} \\ \Gamma_{2,3} \\ \Gamma_{2,4} \end{bmatrix} - \bar{M}_1 \begin{bmatrix} (\alpha_u - \bar{\alpha}_u)/\zeta \\ (\alpha_q - \bar{\alpha}_q)/\zeta \\ (\alpha_r - \bar{\alpha}_r)/\zeta \end{bmatrix} + \begin{bmatrix} \hat{W}_2^\top \Omega_2 \\ \hat{W}_3^\top \Omega_3 \\ \hat{W}_4^\top \Omega_4 \end{bmatrix} + \hat{\varepsilon} \begin{bmatrix} \tanh(\frac{\Gamma_{2,2}}{\vartheta}) \\ \tanh(\frac{\Gamma_{2,3}}{\vartheta}) \\ \tanh(\frac{\Gamma_{2,4}}{\vartheta}) \end{bmatrix} \right) \tag{18}$$

where $\bar{\gamma}_{2,2} = \text{diag}[\gamma_{2,2}, \gamma_{2,3}, \gamma_{2,4}]$; $\gamma_{2,2}$, $\gamma_{2,3}$, and $\gamma_{2,4}$ are the positive design parameters, and

$$\bar{M}_1 = \begin{bmatrix} 0 & 0 & mx_g - Y_{\dot{r}} \\ 0 & -mx_g - z\dot{q} & 0 \\ 0 & 0 & 0 \end{bmatrix}$$

$$\bar{M}_2 = \begin{bmatrix} m - Y_{\dot{\varphi}} & 0 & -mz_g \\ 0 & m - Z_{\dot{w}} & my_g \\ -mz_g & my_g & I_{xx} - K_{\dot{p}} \end{bmatrix}.$$

The adaptive laws for \hat{W}_f , $f = 1, \dots, 6$, and $\hat{\varepsilon}$ are designed as

$$\dot{\hat{W}}_f = \zeta_f (\Gamma_{2,f} \Omega_f - \sigma_1 \hat{W}_f) \tag{19}$$

$$\dot{\hat{\varepsilon}} = \iota \left(\Gamma_2^\top \tanh\left(\frac{\Gamma_2}{\vartheta}\right) - \sigma_2 \hat{\varepsilon} \right) \tag{20}$$

where $f = 1, \dots, 6$, $\tanh(\Gamma_2/\vartheta) = [\tanh(\Gamma_{2,1}/\vartheta), \dots, \tanh(\Gamma_{2,6}/\vartheta)]^\top$, $\zeta_f = \text{diag}[\zeta_{f,1}, \dots, \zeta_{f,n}]$; $\zeta_{f,l} > 0$, $l = 1, \dots, n$ is a constant, ι , σ_1 and σ_2 are positive design constants.

Let us consider a Lyapunov function V_2 as

$$V_2 = \frac{1}{2}\Gamma_2^\top M\Gamma_2 + \frac{1}{2}tr(\tilde{W}^\top \zeta^{-1}\tilde{W}) + \frac{1}{2l}\tilde{\varepsilon}^2 \tag{21}$$

where $\tilde{W} = W^* - \hat{W}$ and $\tilde{\varepsilon} = \bar{\varepsilon} - \hat{\varepsilon}$ are estimation errors, $\zeta = \text{diag}[\zeta_1, \dots, \zeta_6]$, and $tr(\cdot)$ means the trace of the matrix.

By substituting (13) and (14) into the time derivative of (21), \dot{V}_2 is obtained as

$$\dot{V}_2 = \Gamma_2^\top (W^{*\top} \Omega + \varepsilon + \check{\tau} - S_\tau) - \Gamma_2^\top B - tr(\tilde{W}^\top \zeta^{-1}\dot{\tilde{W}}) - \frac{1}{l}\tilde{\varepsilon}\dot{\tilde{\varepsilon}}. \tag{22}$$

It holds that $\Gamma_2^\top S_\tau = e^\top \bar{S}_\tau$ and $\|S_\tau\| = \|\bar{S}_\tau\|$ with $S_\tau = [\check{\tau}_1 - \tau_X, 0, 0, 0, \check{\tau}_5 - \tau_M, \check{\tau}_6 - \tau_N]^\top$ and $\bar{S}_\tau = [\check{\tau}_1 - \tau_X, \check{\tau}_5 - \tau_M, \check{\tau}_6 - \tau_N]^\top$. Then, using the property $S_\tau(t_j) = 0$ for $j \in \mathbb{Z}^+$ and the event-triggering condition (16), we have $-\Gamma_2^\top S_\tau \leq \|e\|(\kappa_1\|e\| + \kappa_2)$.

Then, using $B = [B_1, \dots, B_6]^\top = M\chi$ and the definition of the matrix M , we have

$$\Gamma_2^\top B = \Gamma_2^\top \begin{bmatrix} B_1 \\ 0 \\ 0 \\ 0 \\ B_5 \\ B_6 \end{bmatrix} + \Gamma_2^\top \begin{bmatrix} 0 \\ \bar{M}_1 \begin{bmatrix} (\alpha_u - \bar{\alpha}_u)/\zeta \\ (\alpha_q - \bar{\alpha}_q)/\zeta \\ (\alpha_r - \bar{\alpha}_r)/\zeta \end{bmatrix} + \bar{M}_2 \begin{bmatrix} \dot{\beta}_1 \\ \dot{\beta}_2 \\ \dot{\beta}_3 \end{bmatrix} \\ 0 \\ 0 \end{bmatrix}. \tag{23}$$

Substituting $-\Gamma_2^\top S_\tau \leq \|e\|(\kappa_1\|e\| + \kappa_2)$ and (23) into (22) and using (17) and (18), we obtain

$$\begin{aligned} \dot{V}_2 \leq & -\Gamma_2^\top \gamma_2 \Gamma_2 + \Gamma_2^\top \tilde{W}^\top \Omega - \frac{1}{l}\tilde{\varepsilon}\dot{\tilde{\varepsilon}} - tr(\tilde{W}^\top \zeta^{-1}\dot{\tilde{W}}) + \|e\|\kappa_2 - \kappa_2 e^\top \tanh\left(\frac{e}{\vartheta}\right) \\ & + \|\Gamma_2\|\bar{\varepsilon} - \bar{\varepsilon}\Gamma_2^\top \tanh\left(\frac{\Gamma_2}{\vartheta}\right) + \bar{\varepsilon}\Gamma_2^\top \tanh\left(\frac{\Gamma_2}{\vartheta}\right) - e^\top N^\top \Gamma_1 \end{aligned} \tag{24}$$

where $\gamma_2 = \text{diag}[\gamma_{2,1}, \dots, \gamma_{2,6}]$.

Lemma 2. [39] $0 \leq |s| - s \tanh(s/\vartheta) \leq 0.2785\vartheta$ for $s \in \mathbb{R}$ and any positive constant ϑ .

By substituting (19) and (20) into (24) and using Lemma 2, \dot{V}_2 becomes

$$\dot{V}_2 \leq -\Gamma_2^\top \gamma_2 \Gamma_2 + \sigma_1 tr(\tilde{W}^\top \dot{\tilde{W}}) + \sigma_2 \tilde{\varepsilon}\dot{\tilde{\varepsilon}} - e^\top N^\top \Gamma_1 + 1.671\bar{\varepsilon}\vartheta + 0.8355\kappa_2\vartheta. \tag{25}$$

Remark 2. In the dynamics (2) of the torpedo-shaped UUV, the underactuated control torque vector $\tau = [\tau_X, 0, 0, 0, \tau_M, \tau_N]$ should be designed. That is, the first, fifth, and sixth dynamic equations in (2) only have the control torques τ_X , τ_M , and τ_N , respectively. Thus, the the auxiliary stabilizing signals are required for the state equations for v , ω , and p (i.e., the second, third, and fourth dynamic equations in (2)). In this study, the auxiliary stabilizing signals β_1 , β_2 , and β_3 in (18) are presented to design the underactuated control torque vector $\tau = [\tau_X, 0, 0, 0, \tau_M, \tau_N]$ while ensuring the predefined three-dimensional tracking performance and the stability of the closed-loop system. Because of these auxiliary stabilizing signals, the UUV dynamics (2) is stably controlled by using the only three control inputs τ_X , τ_M , and τ_N .

We analyze the predefined three-dimensional tracking performance and stability of the closed-loop system and the exclusion of Zeno behavior of the proposed event-triggered scheme in the following theorem.

Theorem 1. Consider the kinematics and dynamics of the uncertain UUV (i.e., (1) and (2)). For initial conditions satisfying $V(0) \leq \Delta$ with a constant $\Delta > 0$, the adaptive event-triggered tracking law (17) guarantees that

- (i) all the closed-loop signals are semi-globally uniformly ultimately bounded;
- (ii) the predefined three-dimensional tracking performance is ensured (i.e., $-\delta_{1,i}\mu_i(t) < s_i(t) < \delta_{2,i}\mu_i(t)$, $i = 1, 2, 3, \forall t \geq 0$);
- (iii) there exists an inter-event time $T_m > 0$ such that $|t_{j+1} - t_j| \geq T_m$.

Proof. The dynamics of the boundary layer error c is represented by

$$\dot{c} = -\frac{1}{\xi}c + \Lambda(\Gamma_1, \Gamma_2, c, \hat{W}, \hat{\varepsilon}, \eta_0) \tag{26}$$

where $\eta_0 = [\eta_d^\top, \dot{\eta}_d^\top, \ddot{\eta}_d^\top]^\top$ and $\Lambda = \dot{N}^{-1}\{-\gamma_1\Gamma_1 - H[0 \ v \ w]^\top + R_1^{-1}A(\dot{\eta}_d + \mu^{-1}\dot{\mu}s_1)\} + N^{-1}\{-\gamma_1\dot{\Gamma} - H[0 \ \dot{v} \ \dot{w}]^\top - \dot{H}[0 \ v \ w]^\top + \dot{R}_1^{-1}A(\dot{\eta}_d + \mu^{-1}\dot{\mu}s_1) + R_1^{-1}\dot{A}(\dot{\eta}_d + \mu^{-1}\dot{\mu}s_1) + R_1^{-1}A(\ddot{\eta}_d + \mu^{-1}\dot{\mu}\dot{s}_1 + \dot{\mu}^{-1}\dot{\mu}s_1 + \mu^{-1}\ddot{\mu}s_1)\}$ is a continuous function.

We define the Lyapunov function $V = V_1 + V_2 + (c^\top c)/2$ to prove this theorem. Using (12), (25), and (26), \dot{V} becomes

$$\begin{aligned} \dot{V} \leq & -\Gamma_1^\top \gamma_1 \Gamma_1 - \Gamma_2^\top \gamma_2 \Gamma_2 - \frac{1}{\xi}c^\top c + c^\top \bar{\Lambda} + \sigma_1 tr(\tilde{W}^\top \hat{W}) \\ & - \sigma_2 \bar{\varepsilon}^2 + \sigma_2 \bar{\varepsilon} \bar{\varepsilon} + 1.671 \bar{\varepsilon} \vartheta + 0.8355 \kappa_2 \vartheta. \end{aligned} \tag{27}$$

where $\bar{\Lambda} = \Lambda + N^\top \Gamma_1$ is a continuous function. Using the inequalities $tr(\tilde{W}^\top \hat{W}) \leq -\|\tilde{W}\|_F^2/2 + \bar{W}^2/2$, $\bar{\varepsilon} \bar{\varepsilon} \leq \bar{\varepsilon}^2/2 + \bar{\varepsilon}^2/2$, and $c^\top \bar{\Lambda} \leq \|c\|^2 \|\bar{\Lambda}\|^2 / (2\varphi) + \varphi/2$ with constants $\varphi > 0$, (27) becomes

$$\dot{V} \leq -\Gamma_1^\top \gamma_1 \Gamma_1 - \Gamma_2^\top \gamma_2 \Gamma_2 - \frac{\|c\|^2}{\xi} + \frac{\|c\|^2 \|\bar{\Lambda}\|^2}{2\varphi} - \frac{\sigma_1}{2} \|\tilde{W}\|_F^2 - \frac{\sigma_2}{2} \bar{\varepsilon}^2 + D \tag{28}$$

where $D = (\sigma_1/2)\bar{W}^2 + (\sigma_2/2)\bar{\varepsilon}^2 + \varphi/2 + 1.671\bar{\varepsilon}\vartheta + 0.8355\kappa_2\vartheta$.

Let us define compact sets $\Pi = \{\Gamma_1^\top \Gamma_1 + \Gamma_2^\top M \Gamma_2 + c^\top c + tr(\tilde{\Phi}^\top \zeta^{-1} \tilde{\Phi}) + (1/\iota)\bar{\varepsilon}^2 \leq 2\Delta\}$ and $\Xi = \{\eta_d^\top \eta_d + \dot{\eta}_d^\top \dot{\eta}_d + \ddot{\eta}_d^\top \ddot{\eta}_d \leq \bar{\eta}_0\}$ with a constant $\bar{\eta}_0 > 0$. Then, there exists a constant Λ^* such that $\|\bar{\Lambda}\| \leq \Lambda^*$ on $\Pi \times \Xi$. By selecting $1/\xi = \zeta^* + (\Lambda^*)^2 / (2\varphi) + 1$ with a constant $\zeta^* > 0$, we have

$$\dot{V} \leq -\Psi V - \left(1 - \frac{\|\bar{\Lambda}\|^2}{(\Lambda^*)^2}\right) \frac{\|c\|^2 (\Lambda^*)^2}{2\varphi} + D \tag{29}$$

where $\Psi = \min[2\gamma_1, 2\gamma_2, 2\zeta^*, \sigma_1 \zeta_{min}, \sigma_2 \iota]$; ζ_{min} is the minimum eigenvalue of ζ . Because of $\|\bar{\Lambda}\| \leq \Lambda^*$ on $V = \Delta$, $\dot{V} \leq -\Psi V + D$ is satisfied on $V = \Delta$. Then, it is ensured that $\dot{V} < 0$ on $V = \Delta$ when $\Psi > D/\Delta$ and thus $V \leq \Delta$ denotes an invariant set. It is proved that all closed-loop signals are semi-global uniform ultimate bounded. This completes the proof of Theorem 1—(i).

By integrating $\dot{V} \leq -\Psi V + D$ with respect to time, we have $V(t) \leq e^{-\Psi t} V(0) + (D/\Psi)[1 - e^{-\Psi t}]$. Using $(1/2)\|\Gamma_1\|^2 \leq V(t)$, it holds that $\lim_{t \rightarrow \infty} \|\Gamma_1\| \leq \sqrt{2D/\Psi}$. That is, Γ_1 is bounded (i.e., $\Gamma_{1,i} \in \mathcal{L}_\infty, i = 1, 2, 3$). From Lemma 1, the predefined three-dimensional tracking performance is ensured (i.e., $-\delta_{1,i}\mu_i(t) < s_i(t) < \delta_{2,i}\mu_i(t), i = 1, 2, 3, \forall t \geq 0$). This completes the proof of Theorem 1—(ii).

To show the exclusion of Zeno behavior of the proposed event-triggering scheme, we prove that there exists a minimum value T_m of inter-event times such that $|t_{j+1} - t_j| \geq T_m$ for $j \in \mathbb{Z}^+$.

For all $t \in [t_j, t_{j+1})$, we consider

$$\frac{d}{dt} \|S_\tau\| = \frac{d}{dt} (S_\tau^\top S_\tau)^{\frac{1}{2}} = \frac{S_\tau^\top \dot{S}_\tau}{\|S_\tau\|} \leq \left\| \frac{d}{dt}(\check{\tau}) \right\| \tag{30}$$

where $\frac{d}{dt}(\check{\tau}) = [\check{\tau}_1, 0, 0, \check{\tau}_5, \check{\tau}_6]^\top$; $\check{\tau}_1$, $\check{\tau}_5$, and $\check{\tau}_6$ are given by

$$\begin{aligned} \begin{bmatrix} \check{\tau}_1 \\ \check{\tau}_5 \\ \check{\tau}_6 \end{bmatrix} &= -\tilde{\gamma}_{2,1} \dot{e} + \begin{bmatrix} \dot{B}_1 \\ \dot{B}_5 \\ \dot{B}_6 \end{bmatrix} - \begin{bmatrix} \hat{W}_1^\top \Omega_1 + \hat{W}_1^\top \dot{\Omega}_1 \\ \hat{W}_5^\top \Omega_5 + \hat{W}_5^\top \dot{\Omega}_5 \\ \hat{W}_6^\top \Omega_6 + \hat{W}_6^\top \dot{\Omega}_6 \end{bmatrix} - \hat{\varepsilon} \tanh\left(\frac{e}{\vartheta}\right) \\ &\quad - (\hat{\varepsilon} + \kappa_2) \left(1 - \tanh^2\left(\frac{e}{\vartheta}\right)\right) \frac{e}{\vartheta} - \kappa_1 \dot{e} - \dot{N}^\top \Gamma_1 - N^\top \dot{\Gamma}_1. \end{aligned} \tag{31}$$

From the boundedness of all the closed-loop signals, there exists a constant $d > 0$ such that $\|\frac{d}{dt}(\check{\tau})\| \leq d$. Integrating $\frac{d}{dt} \|S_\tau\| \leq d$ during $t \in [t_j, t_{j+1})$ and using the event-triggering condition (16) yield $|t_{j+1} - t_j| \geq (\kappa_1 \|e(t)\| + \kappa_2) / d \geq \kappa_2 / d$. By defining $T_m = \kappa_2 / d$, it holds that $|t_{j+1} - t_j| \geq T_m$. This completes the proof of Theorem 1—(iii). \square

4. Simulation Examples

The parameters of the UUV are borrowed from [35]. The reference signal is given by $\eta_d(t) = [30 \cos(0.15t), 30 \sin(0.15t), 2t]^\top$ and the initial position of the UUV is set to $\eta(0) = [45, 5, 5]$. The control parameters of the UUV are chosen as $\gamma_1 = \text{diag}[1.0, 1.0, 1.0]$, $\gamma_2 = \text{diag}[50, 30, 30, 30, 50, 50]$, $\zeta_{f,l} = 30$, $\iota = 30$, $\sigma_1 = 0.05$, $\sigma_2 = 0.05$, $\xi = 0.05$, $\vartheta = 0.1$, and $\varrho = -0.1$ where $f = 1, \dots, 6$ and $l = 1, \dots, n$. The parameters for performance functions are selected as $\delta_{1,1} = 0.75$, $\delta_{2,1} = 1.0$, $\delta_{1,2} = 0.7$, $\delta_{2,2} = 0.7$, $\delta_{1,3} = 0.7$, $\delta_{2,3} = 0.7$, $g_1 = 1.1$, $g_2 = 1.05$, $g_3 = 1.0$, $\mu_{1,0} = 30$, $\mu_{1,\infty} = 2$, $\mu_{2,0} = 10$, $\mu_{2,\infty} = 1$, $\mu_{3,0} = 10$, and $\mu_{3,\infty} = 1$. For the event-triggering condition, we set $\kappa_1 = 100$ and $\kappa_2 = 1$. The event-triggering condition is checked every the sampling time 0.005 s.

The three-dimensional tracking result is shown in Figure 2. In Figure 2, the UUV follows the desired trajectory with good performance. Figure 3 depicts the position tracking errors. Figure 3 reveals that the time responses of the position errors s_i remain within the predefined time-varying performance bounds $-\delta_{1,i}\mu_i$ and $\delta_{2,i}\mu_i$ for all $t \geq 0$. The mean square errors of the position errors s_i at the steady-state response are presented in Table 1 where the steady-state response is set to the position errors $s_i(t)$ for $t \geq 10$ s. The outputs of the neural networks are displayed in Figure 4. The event-triggered underactuated control inputs for the UUV are shown in Figure 5. Figure 6 shows the triggered time intervals and the cumulative number of events of the proposed event-triggered control laws. The number of total events of the proposed event-triggered tracker is 2164. Thus, the data required for implementing the proposed tracker are only 18.03% of the total sampled data 12,000 during 60 s. This implies that the proposed event-triggered control scheme can save the signal transmission burden. From these results, we can see that predefined three-dimensional tracking performance under the underactuated property of the uncertain nonlinear 6-DOF UUV can be achieved by the proposed adaptive event-triggered tracking methodology.

Table 1. Mean square errors of $s_1(t)$, $s_2(t)$, and $s_3(t)$ at the steady-state response.

s_1	s_2	s_3
0.0177	0.0052	4.0268×10^{-4}

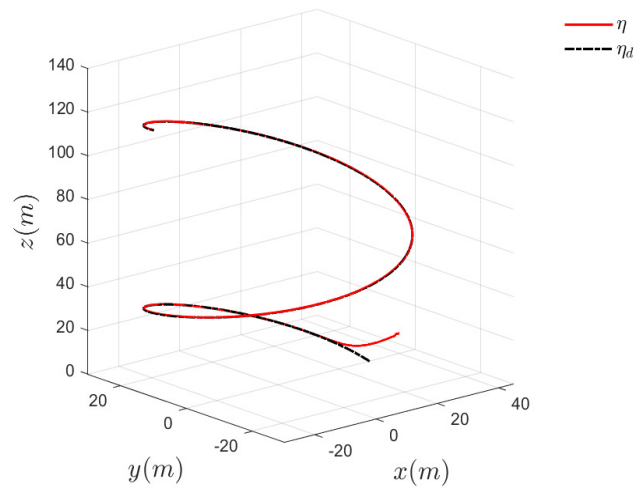


Figure 2. Three-dimensional tracking result.

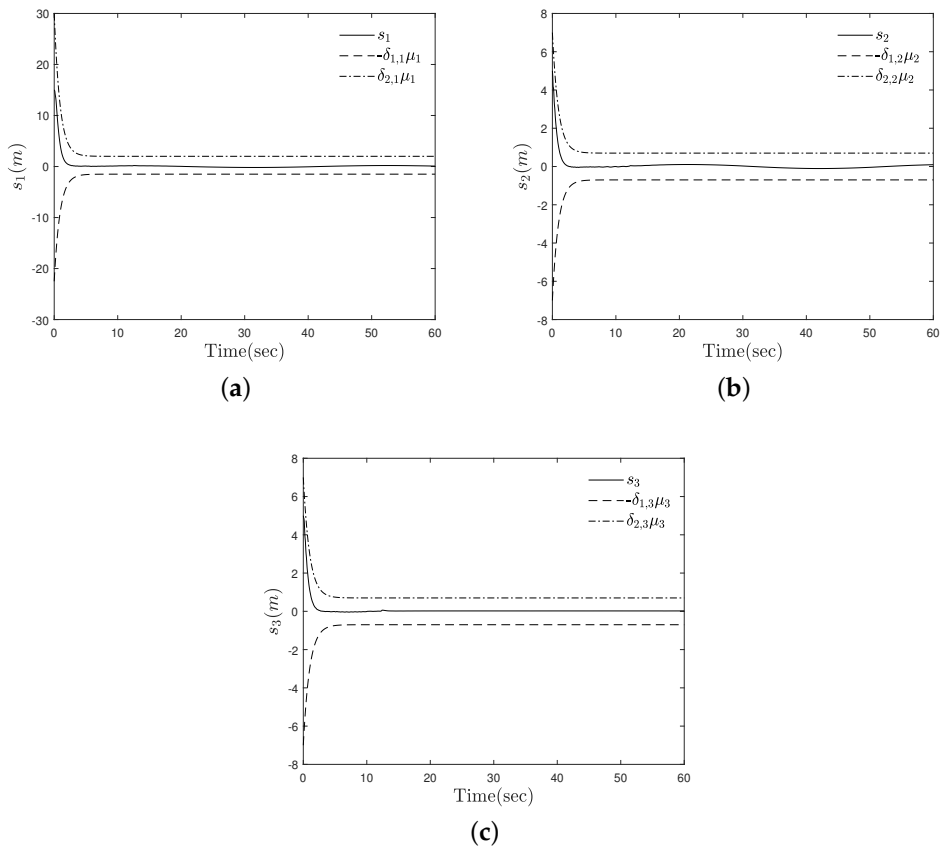


Figure 3. Tracking errors and performance bounds (a) s_1 , $-\delta_{1,1}\mu_1$, and $\delta_{2,1}\mu_1$ (b) s_2 , $-\delta_{1,2}\mu_2$, and $\delta_{2,2}\mu_2$ (c) s_3 , $-\delta_{1,3}\mu_3$, and $\delta_{2,3}\mu_3$.

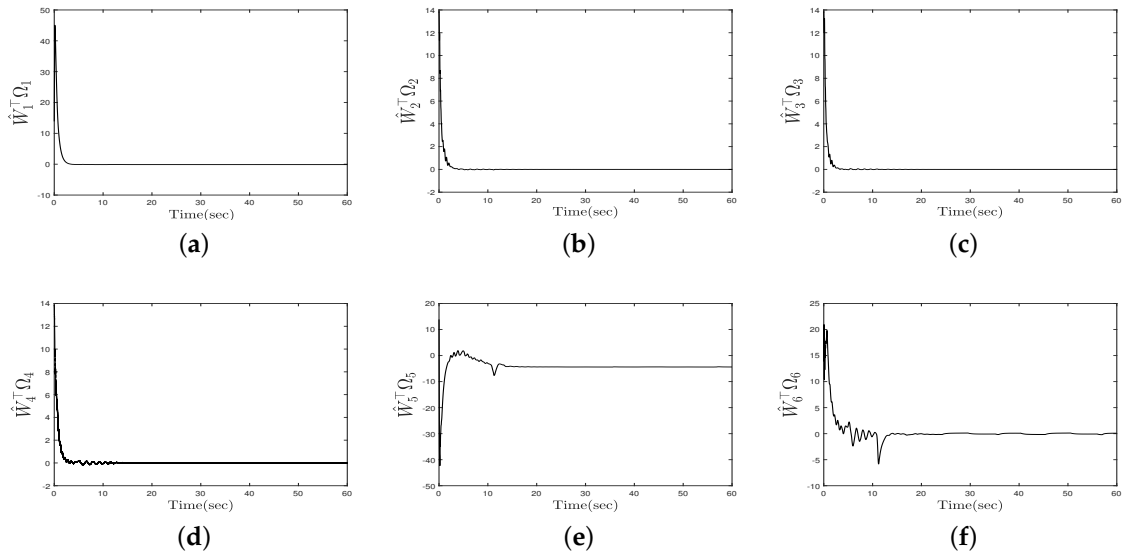


Figure 4. Outputs of neural networks (a) $W_1\Omega_1$ (b) $W_2\Omega_2$ (c) $W_3\Omega_3$ (d) $W_4\Omega_4$ (e) $W_5\Omega_5$ (f) $W_6\Omega_6$.

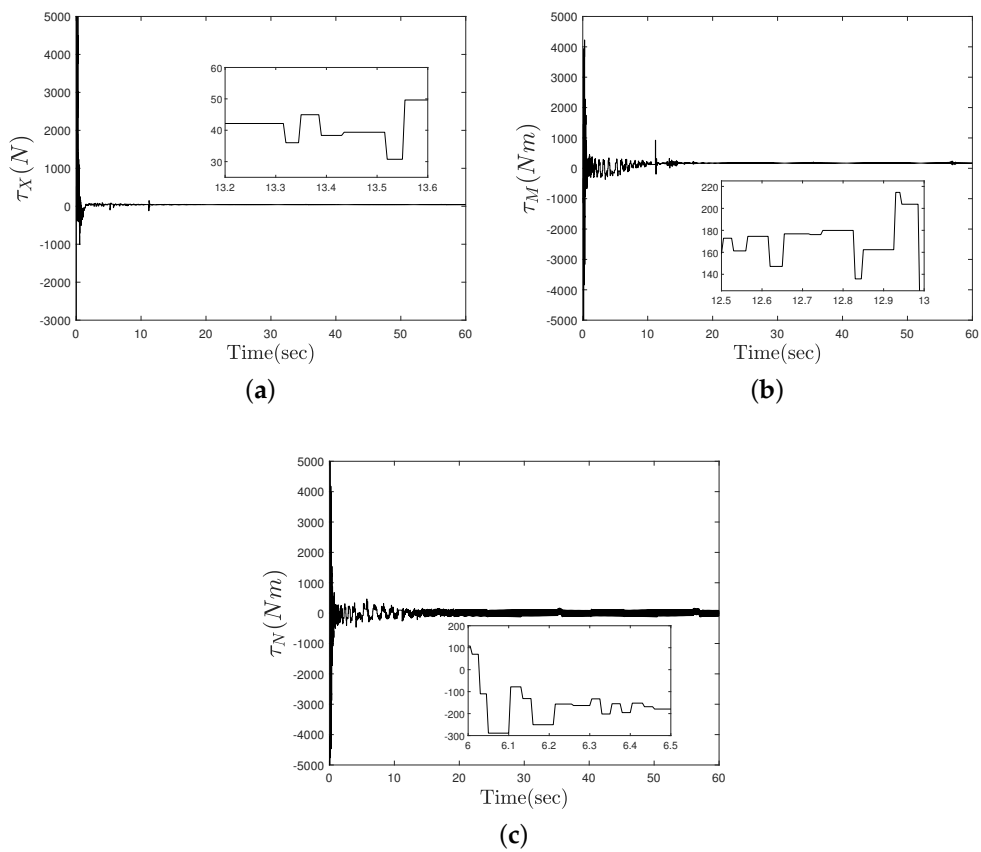


Figure 5. Event-triggered control laws (a) τ_X (b) τ_M (c) τ_N .

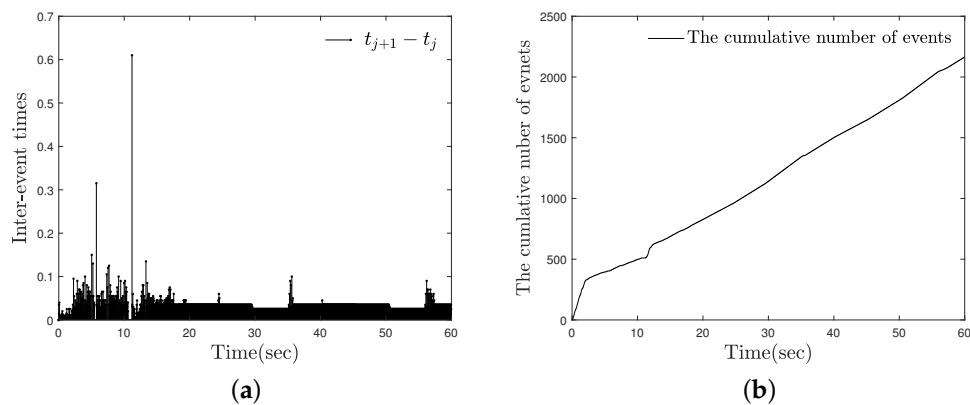


Figure 6. Inter-event times and the cumulative number of events (a) inter-event times (b) the cumulative number of events.

5. Conclusions

We presented an adaptive event-triggered control method for ensuring predefined three-dimensional tracking performance of uncertain nonlinear 6-DOF UUVs. The nonlinearly transformed error function and the auxiliary stabilizing signals were derived for achieving predefined three-dimensional tracking performance while overcoming the underactuated problem of the nonlinear 6-DOF dynamics. It was shown that the adaptive event-triggered tracker using neural networks achieves the practical stability and predefined tracking performance of the closed-loop system. The main contribution of this work to the event-triggered control of uncertain nonlinear 6-DOF UUVs is that the predefined three-dimensional tracking performance under the underactuated dynamics can be admitted than the conventional event-triggered techniques of underwater vehicles in the two-dimensional space.

Author Contributions: Conceptualization, methodology, software, writing—original draft preparation, J.H.K.; Conceptualization, methodology, writing—review and editing, supervision, S.J.Y. All authors have read and agreed to the published version of the manuscript.

Funding: This research was supported by the National Research Foundation of Korea (NRF) grant funded by the Korea government (NRF-2019R1A2C1004898).

Institutional Review Board Statement: Not applicable.

Informed Consent Statement: Not applicable.

Data Availability Statement: Not applicable.

Conflicts of Interest: The authors declare no conflict of interest.

Appendix A

The matrices M_1 and M_2 , and the vectors $G(\zeta)$ and $C(v, \omega)$ of the dynamics (2) are defined as [35]

$$M_1 = \begin{bmatrix} m & 0 & 0 & 0 & mz_g & -my_g \\ 0 & m & 0 & -mz_g & 0 & mx_g \\ 0 & 0 & m & my_g & -mx_g & 0 \\ 0 & -mz_g & my_g & I_{xx} & 0 & 0 \\ mz_g & 0 & -mx_g & 0 & I_{yy} & 0 \\ -my_g & mx_g & 0 & 0 & 0 & I_{zz} \end{bmatrix}$$

$$M_2 = \begin{bmatrix} -X_{\dot{u}} & 0 & 0 & 0 & 0 & 0 \\ 0 & -Y_{\dot{v}} & 0 & 0 & 0 & -Y_{\dot{r}} \\ 0 & 0 & -Z_{\dot{w}} & 0 & -Z_{\dot{q}} & 0 \\ 0 & 0 & 0 & -K_{\dot{p}} & 0 & 0 \\ 0 & 0 & -M_{\dot{w}} & 0 & -M_{\dot{q}} & 0 \\ 0 & -N_{\dot{v}} & 0 & 0 & 0 & -N_{\dot{r}} \end{bmatrix}$$

$$G(\zeta) = \begin{bmatrix} -(W - F)s_{\theta} \\ (W - F)c_{\theta}s_{\phi} \\ (W - F)c_{\theta}c_{\phi} \\ -(y_g W - y_b F)c_{\theta}c_{\phi} - (z_g W - z_b F)c_{\theta}s_{\phi} \\ -(z_g W - z_b F)s_{\theta} - (x_g W - x_b F)c_{\theta}c_{\phi} \\ -(x_g W - x_b F)c_{\theta}s_{\phi} - (y_g W - y_b F)s_{\theta} \end{bmatrix}$$

$$C(v, \omega) = [C_1, \dots, C_6]^T$$

$$C_1 = X_{|u|u}|u|u| + (X_{wq} - m)\omega q + (X_{qq} + mx_g)q^2 + (X_{vr} + m)vr + (X_{rr} + mx_g)r^2 - my_g pq - mz_g pr$$

$$C_2 = Y_{|v|v}|v|v| + Y_{r|r}|r|r| + my_g r^2 + (Y_{ur} - m)ur + Y_{uv}uv + (Y_{wp} + m)wp + (Y_{pq} - mx_g)pq + my_g p^2 + mz_g qr$$

$$C_3 = Z_{|w|w}|w|w| + Z_{q|q}|q|q| + (Z_{uq} + m)uq + (Z_{vp} - m)vp + (Z_{rp} - mx_g)rp + Z_{uw}u\omega + mz_g(p^2 + q^2) - my_g rq$$

$$C_4 = K_{p|p}|p|p| - (I_{zz} - I_{yy})qr + my_g(uq - vp) - mz_g(wp - ur)$$

$$C_5 = M_{|w|w}|w|w| + M_{q|q}|q|q| + (M_{uq} - mx_g)uq + (M_{vp} + mx_g)vp + (M_{rp} - (I_{xx} - I_{zz}))rp + mz_g(vr - \omega q) + M_{uw}u\omega$$

$$C_6 = N_{|v|v}|v|v| + N_{r|r}|r|r| + (N_{ur} - mx_g)ur + (N_{wp} + mx_g)wp + (N_{pq} - (I_{yy} - I_{xx}))pq - my_g(vr - \omega q) + N_{uv}uv$$

where m is the mass of the UUV, $x_g, y_g,$ and z_g mean the center of gravity of the UUV, $x_b, y_b,$ and z_b represent the center of buoyancy of the UUV, the vehicle weight and the vehicle buoyancy of the UUV are defined as W and F , respectively, $I_{xx}, I_{yy},$ and I_{zz} denote the inertia tensors of the UUV, $X_{\dot{u}}, Y_{\dot{v}}, Y_{\dot{r}}, Z_{\dot{w}}, Z_{\dot{q}}, K_{\dot{p}}, M_{\dot{w}}, M_{\dot{q}}, N_{\dot{r}},$ and $N_{\dot{v}}$ are the added mass parameters of the UUV, $X_{vr}, X_{wq}, X_{qq}, X_{rr}, Y_{ur}, Y_{wp}, Y_{pq}, Y_{uv}, Z_{uq}, Z_{vp}, Z_{rp}, Z_{uw}, M_{uq}, M_{vp}, M_{rp}, M_{uw}, N_{ur}, N_{wp}, N_{pq},$ and N_{uv} indicate the parameters of the added mass cross term of the UUV, $X_{|u|u}$ is the axial drag parameter of the UUV, and the cross flow drag parameters of the UUV are defined as $Y_{|v|v}, Y_{r|r}, Z_{|w|w}, Z_{q|q}, K_{|p|p}, M_{|w|w}, M_{q|q}, N_{|v|v},$ and $N_{r|r}$.

References

1. Yuh, J. Design and control of autonomous underwater robots: A survey. *Auton. Robot.* **2000**, *8*, 7–24. [CrossRef]
2. Bellingham, J.G.; Rajan, K. Robotics in remote and hostile environments. *Science* **2007**, *318*, 1098–1102. [CrossRef] [PubMed]
3. Farrell, J.A.; Li, W.; Pang, S.; Arrieta, R. Chemical plume tracing experimental results with REMUS AUV. *Oceans* **2003**, *2*, 962–968.
4. Peymani, E.; Fossen, T.I. Path following of underwater robots using lagrange multipliers. *Robot. Auton. Syst.* **2015**, *67*, 44–52. [CrossRef]
5. Sahoo, A.; Dwivedy, S.K.; Robi, P. Advancements in the field of autonomous underwater vehicle. *Ocean Eng.* **2019**, *181*, 145–160. [CrossRef]
6. Ribas, D.; Palomeras, N.; Ridao, P.; Carreras, M.; Mallios, A. Girona 500 auv: From survey to intervention. *IEEE/ASME Trans. Mechatron.* **2012**, *17*, 46–53. [CrossRef]
7. Li, J.H.; Lee, P.M. Design of an adaptive nonlinear controller for depth control of an autonomous underwater vehicle. *Ocean Eng.* **2005**, *32*, 2165–2181. [CrossRef]

8. Shen, C.; Shi, Y.; Buckham, B. Trajectory tracking control of an autonomous underwater vehicle using Lyapunov-based model predictive control. *IEEE Trans. Ind. Electron.* **2018**, *65*, 5796–5805. [[CrossRef](#)]
9. Taha, E.; Mohamed, Z.; Kamal, Y. Terminal sliding mode control for the trajectory tracking of underactuated Autonomous Underwater Vehicles. *Ocean Eng.* **2017**, *129*, 613–625.
10. Repoulas, F.; Papadopoulos, E. Planar trajectory planning and tracking control design for underactuated AUVs. *Ocean Eng.* **2007**, *34*, 1650–1667. [[CrossRef](#)]
11. Cho, G.R.; Li, J.H.; Park, D.; Jung, J.H. Robust trajectory tracking of autonomous underwater vehicles using back-stepping control and time delay estimation. *Ocean Eng.* **2020**, *201*, 107131. [[CrossRef](#)]
12. Liang, X.; Qu, X.; Hou, Y.; Zhang, J. Three-dimensional path following control of underactuated autonomous underwater vehicle based on damping backstepping. *Int. J. Adv. Robot. Syst.* **2017**, *14*, 1729881417724179. [[CrossRef](#)]
13. Liang, X.; Qu, X.; Hou, Y.; Ma, Q. Three-dimensional trajectory tracking control of an underactuated autonomous underwater vehicle based on ocean current observer. *Int. J. Adv. Robot. Syst.* **2018**, *15*, 1729881418806811. [[CrossRef](#)]
14. Wang, J.; Wang, C.; Wei, Y.; Zhang, C. Three-dimensional path following of an underactuated AUV based on neuro-adaptive command filtered backstepping control. *IEEE Access* **2018**, *6*, 74355–74365. [[CrossRef](#)]
15. Shojaei, K. Three-dimensional neural network tracking control of a moving target by underactuated autonomous underwater vehicles. *Neural Comput. Appl.* **2019**, *31*, 509–521. [[CrossRef](#)]
16. Karkoub, M.; Wu, H.M.; Hwang, C.L. Nonlinear trajectory-tracking control of an autonomous underwater vehicle. *Ocean Eng.* **2017**, *145*, 188–198. [[CrossRef](#)]
17. Rezazadegan, F.; Shojaei, K.; Sheikholeslam, F.; Chatraei, A. A novel approach to 6-DOF adaptive trajectory tracking control of an AUV in the presence of parameter uncertainties. *Ocean Eng.* **2015**, *107*, 246–258. [[CrossRef](#)]
18. Chu, Z.; Xiang, X.; Zhu, D.; Luo, C.; Xie, D. Adaptive fuzzy sliding mode diving control for autonomous underwater vehicle with input constraint. *Int. J. Fuzzy Syst.* **2018**, *20*, 1460–1469. [[CrossRef](#)]
19. Bechlioulis, C.P.; Rovithakis, G.A. Robust adaptive control of feedback linearizable MIMO nonlinear systems with prescribed performance. *IEEE Trans. Autom. Control* **2008**, *53*, 532–538. [[CrossRef](#)]
20. Elhaki, O.; Shojaei, K. A robust neural network approximation-based prescribed performance output-feedback controller for autonomous underwater vehicles with actuators saturation. *Eng. Appl. Art. Int.* **2020**, *88*, 103382. [[CrossRef](#)]
21. Liu, X.; Zhang, M.; Wang, S. Adaptive region tracking control with prescribed transient performance for autonomous underwater vehicle with thruster fault. *Ocean Eng.* **2020**, *196*, 106804. [[CrossRef](#)]
22. Elhaki, O.; Shojaei, K. Neural network-based target tracking control of underactuated autonomous underwater vehicles with a prescribed performance. *Ocean Eng.* **2018**, *167*, 239–256. [[CrossRef](#)]
23. Bechlioulis, C.P.; Karras, G.C.; Heshmati-Alamdari, S.; Kyriakopoulos, K.J. Trajectory tracking with prescribed performance for underactuated underwater vehicles under model uncertainties and external disturbances. *IEEE Trans. Control Syst. Technol.* **2017**, *25*, 429–440. [[CrossRef](#)]
24. Campos, R.; Gracias, N.; Ridao, P. Underwater multi-vehicle trajectory alignment and mapping using acoustic and optical constraints. *Sensors* **2016**, *16*, 387. [[CrossRef](#)] [[PubMed](#)]
25. Brockett, R.W.; Liberzon, D. Quantized feedback stabilization of linear systems. *IEEE Trans. Autom. Control* **2000**, *45*, 1279–1289. [[CrossRef](#)]
26. Mazo, M.; Tabuada, P. Decentralized event-triggered control over wireless sensor/actuator networks. *IEEE Trans. Autom. Control* **2011**, *56*, 2456–2461. [[CrossRef](#)]
27. Li, F.; Gao, L.; Dou, G.; Zheng, B. Dual-side event-triggered output feedback H_∞ control for NCS with communication delays. *Int. J. Control Autom. Syst.* **2018**, *16*, 108–119. [[CrossRef](#)]
28. Tallapragada, P.; Chopra, N. On event triggered tracking for nonlinear systems. *IEEE Trans. Autom. Control* **2013**, *58*, 2343–2348. [[CrossRef](#)]
29. Xing, L.; Wen, C.; Liu, Z.; Su, H.; Cai, J. Adaptive compensation for actuator failures with event-triggered input. *Automatica* **2017**, *85*, 129–136. [[CrossRef](#)]
30. Ma, H.; Li, H.; Liang, H.; Dong, G. Adaptive fuzzy event-triggered control for stochastic nonlinear systems with full state constraints and actuator faults. *IEEE Trans. Fuzzy Syst.* **2019**, *27*, 2242–2254. [[CrossRef](#)]
31. Qiu, J.; Sun, K.; Wang, T.; Gao, H. Observer-based fuzzy adaptive event-triggered control for pure-feedback nonlinear systems with prescribed performance. *IEEE Trans. Fuzzy Syst.* **2019**, *27*, 2152–2162. [[CrossRef](#)]
32. Wang, J.; Liu, Z.; Zhang, Y.; Chen, C.L.P. Neural adaptive event-triggered control for nonlinear uncertain stochastic systems with unknown hysteresis. *IEEE Trans. Neural Netw. Learn. Syst.* **2019**, *30*, 3300–3312. [[CrossRef](#)] [[PubMed](#)]
33. Batmani, Y.; Najafi, S. Event-triggered H_∞ depth control of remotely operated underwater vehicles. *IEEE Trans. Syst. Man Cybern. Syst.* **2019**. [[CrossRef](#)]
34. Bian, J.; Xiang, J. Three-dimensional coordination control for multiple autonomous underwater vehicles. *IEEE Access* **2019**, *7*, 63913–63920 [[CrossRef](#)]
35. Presterro, T. Verification of a Six-Degree of Freedom Simulation Model for the REMUS Autonomous Underwater Vehicles. Ph.D. Thesis, Department of Mechanical Engineering, Massachusetts Institute of Technology, Cambridge, MA, USA, 2001.
36. Fossen, T. *Handbook of Marine Craft Hydrodynamics and Motion Control*; John Wiley and Sons, Ltd.: Chichester, UK, 2011.

-
37. Yoo, S.J. Fault-tolerant control of strict-feedback non-linear time-delay systems with prescribed performance. *IET Control Theory Appl.* **2013**, *7*, 1553–1561. [[CrossRef](#)]
 38. Swaroop, D.; Hedrick, J.; Yip, P.P.; Gerdes, J. Dynamic surface control for a class of nonlinear systems. *IEEE Trans. Autom. Control* **2000**, *45*, 1893–1899. [[CrossRef](#)]
 39. Polycarpou, M.M. Stable adaptive neural control scheme for nonlinear systems. *IEEE Trans. Autom. Control* **1996**, *41*, 447–451. [[CrossRef](#)]